

Membrane Protein Microarrays

Ye Fang, Anthony G. Frutos, and Joydeep Lahiri*

Biochemical Technologies, Science and Technology Division, Corning Incorporated, Corning, New York 14831

Received October 22, 2001

This paper describes the fabrication of arrays of G protein-coupled receptors (GPCRs)¹ and assays for screening of ligands on these arrays. The attractiveness of obtaining large amounts of bioinformation² using extremely small volumes of samples has inspired the extension of DNA microarray technology to proteins.³ There are two important reasons for the complementary development of protein microarrays: (i) analysis of protein expression from mRNA levels using DNA microarrays is prone to artifacts and does not provide information regarding posttranslational modifications; (ii) proteins are the molecular entities that bind drugs; hence, the analysis of protein–drug interactions provides direct information about compound design and selectivity. Although there have been several reports on protein microarrays,⁴ there are no reports describing membrane protein arrays and their use for ligand screening.⁵ Membrane-bound proteins represent the single most important class of drug targets—approximately 50% of current molecular targets are membrane-bound.⁶ Therefore, the lack of microarray methods for membrane proteins is viewed as a fundamental limitation of protein microchip technology.

Arraying membrane proteins requires printing mixtures of the protein and associated lipids, which in turn warrants appropriate surface chemistry for the immobilization of lipids. We investigated the structure and properties of supported lipids on several surfaces and found that surfaces modified with γ -aminopropylsilane (GAPS)⁷ uniquely provided the desired combination of properties for supported lipids, as described below. Membrane microspots on GAPS were obtained by printing vesicular solutions of dipalmitoylphosphatidylcholine (DPPC)/dimyristylphosphatidylcholine (DMPC) (4:1) or egg-yolk PC doped with 1% Texas-Red labeled dihexadecanoylphosphatidylethanolamine (TR-DHPE) on slides, using a quill-pin printer.^{8,9} At room temperature, DPPC/DMPC lipids are in the gel-phase and egg-yolk PC is in the fluid phase. Figure 1A shows fluorescence images of lipid microspots on GAPS slides that were subjected to repeated immersion in buffer and withdrawal through the air–buffer interface. Remarkably, no loss in the fluorescence intensity of the microspots was observed. When similar experiments were performed on lipid microspots printed on bare-glass substrates, significant loss of signal was observed. Boxer and co-workers have reported that supported lipids on bare glass spontaneously desorb when withdrawn through air–water interfaces.¹⁰ Our observations suggest that printed lipid microspots on GAPS slides have high mechanical stability, independent of the phase of the lipid.¹¹

We probed the long-range lateral fluidity of supported membranes on GAPS slides using fluorescence recovery after photobleaching (FRAP) experiments.¹² In these experiments, a GAPS slide was incubated with a vesicular solution of dilaurylphosphatidylcholine (DLPC) (doped with TR-DHPE) to form a supported membrane. Figure 1B shows the partial recovery of a photobleached spot in the supported membrane, suggesting long-range fluidity; analysis of the images reveals that the photobleached spot recovers

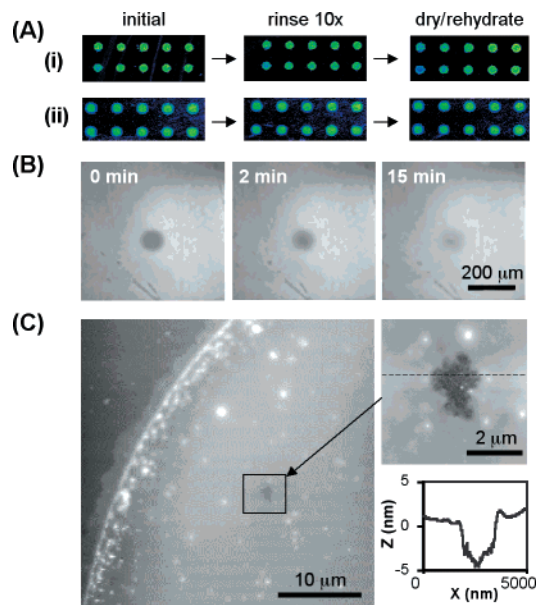


Figure 1. Characterization of model lipid arrays. (A) In situ fluorescence images of microarrays of (i) DPPC/DMPC (4:1 mol ratio) lipids and (ii) egg-yolk PC lipids, doped with TR-DHPE (1%, mol %) on GAPS slides. After printing, the arrays were immersed in buffer and imaged to obtain the initial image. The arrays were then rinsed 10 times by repeated immersions in buffer and withdrawal through the air–buffer interface. Finally, the arrays were dried and rehydrated by immersion in buffer. (B) Fluorescence images of supported membranes of DLPC doped with 1% TR-DHPE on a GAPS slide from a FRAP experiment (0, 2, and 15 min after photobleaching for 2 min). (C) AFM image of a DLPC microspot printed on a GAPS-coated slide.

~50% after bleaching. A parallel experiment on a bare-glass substrate showed ~90% recovery in the same time period (15 min). These results suggest that supported membranes on GAPS slides have reduced mobility relative to supported membranes on bare glass, consistent with the observation of Shen et al.¹³

Atomic force microscopy (AFM)¹⁴ was used to examine the structure of lipid microspots on GAPS. Figure 1C shows an AFM image of a portion of a DLPC spot on GAPS. The image shows a smooth surface with raised edges at the microspot/substrate boundary, suggesting a uniform distribution of lipids across the bulk of the spot. The inset shows a height profile of the supported lipid using a defect site as a reference; significantly, the height difference is ~5 nm, which corresponds to the height of a single supported lipid bilayer.^{13,15}

To demonstrate the feasibility of fabricating arrays of real biological membranes containing membrane-bound receptors, we printed GPCRs. Figure 2A shows fluorescence false-color images of five separate arrays of three GPCRs printed on a GAPS slide. These GPCRs are the adrenergic receptor (β 1), the neurotensin receptor (NTR1) and the dopamine (D1) receptor. The first array (Figure 2A (i)) was incubated with the binding buffer only. As expected, no fluorescence is observed. The second array (Figure

* To whom correspondence should be addressed. Email: lahiri@corning.com.

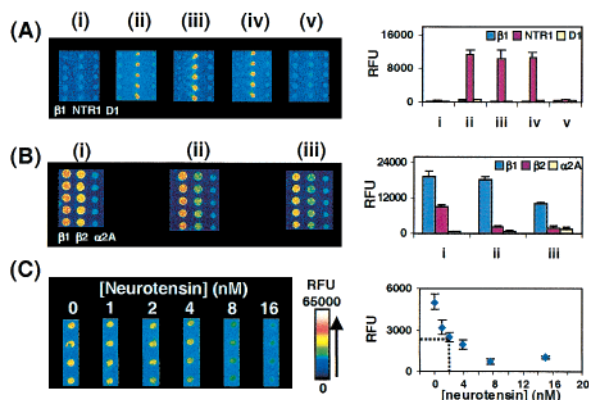


Figure 2. Ligand binding to GPCR microarrays. (A) Fluorescence images and histogram analysis of ligand binding to arrays of the $\beta 1$, NTR1, and D1 receptors on a GAPS slide. Each array contains three columns (each corresponding to a different receptor) of five replicate microspots. Five separate arrays are shown after incubation with (i) binding buffer (50 mM Tris-HCl, 2 mM EDTA, 1 mM $MgCl_2$, pH 7.4, 0.1% BSA) only; (ii) BT-NT (2 nM); (iii)–(v) BT-NT (2 nM) in the presence of CGP12177 (1 μM), SCH23390 (1 μM) and neurotensin (1 μM), respectively. Error bars in the histogram represent the standard deviation of five replicate microspots. (B) Fluorescence images and histogram analysis of ligand binding to arrays of the adrenergic receptor. Three separate arrays of the $\beta 1$, $\beta 2$, and $\alpha 2A$ receptors were printed on a single GAPS-coated gold slide. The arrays were incubated with (i) BT-CGP (5 nM) only, (ii) BT-CGP (5 nM) and ICI 11851 (10 nM), (iii) BT-CGP (5 nM) and ICI 11851 (500 nM). (C) Fluorescence images and inhibition curve of arrays of the NTR1 receptor. The arrays were incubated in solutions containing a fixed concentration of BT-NT (1 nM) and different concentrations of neurotensin (0–16 nM). The dotted line in the graph corresponds to the estimated IC_{50} value of ~ 2 nM.

2A (ii)) was incubated with a solution containing fluorescently labeled neurotensin (Bodipy-TMR-neurotensin (BT-NT)). The image reveals that only the array corresponding to NTR1 shows a strong fluorescence signal; this observation suggests that the binding of BT-NT to NTR1 is specific. The specificity of the interaction was further demonstrated by incubating the arrays with solutions containing BT-NT and either CGP 12177, SCH 23390, or neurotensin (Figure 2A (iii), (iv), (v), respectively). Relative to arrays incubated with BT-NT, there is no significant decrease in signals for arrays incubated with mixtures containing BT-NT and CGP 12177 or SCH 23390. These ligands have no known affinity for NTR1 and are not expected to inhibit the binding of BT-NT to NTR1. Neurotensin is the cognate ligand for NTR1 ($K_i \approx 2.0$ nM)¹⁶ and competes for binding sites on the NTR1 array. Therefore, when incubated with solutions containing excess neurotensin, complete inhibition is expected, in accordance with the data.

Protein microarrays are particularly well-suited for determining the selectivity of a compound between the different subtypes of a receptor family. To test this application, we printed arrays containing different adrenergic receptors and carried out binding assays with labeled cognate ligands and unlabeled inhibitors. GAPS-derivatized gold surfaces¹⁷ were used for this experiment because of background issues related to nonspecific binding of fluorescent ligands on the glass substrates. We hypothesized that distance-dependent quenching by the gold surface would decrease the fluorescence due to nonspecific binding outside the microspots relative to binding within the microspots.¹⁸ Each array contained the $\beta 1$, $\beta 2$, and $\alpha 2A$ subtypes of the adrenergic receptor. The first array was incubated with Bodipy-TMR CGP 12177, a β -selective antagonist analogue.¹⁹ Figure 2B (i) shows a fluorescence image of this array; only spots corresponding to the $\beta 1$ and $\beta 2$ subtypes show binding to CGP12177, in agreement with the known selectivity of this compound. The arrays were incubated with solutions containing labeled CGP 12177 and ICI 118551, a selective $\beta 2$ antagonist,²⁰ at

two different concentrations (shown in Figure 2B, (ii) and (iii), respectively). At 10 nM ICI 118551, we observed decreases of 75 and 6% in the fluorescence intensity of the spots corresponding to the $\beta 2$ receptor and the $\beta 1$ receptor, respectively. When the concentration of ICI 118551 was increased to 500 nM, the fluorescence intensities of the spots of the $\beta 1$ receptor decreased to approximately 48% and no further decrease was observed for spots of the $\beta 2$ receptor. These results are consistent with the higher affinity of ICI 118551 for the $\beta 2$ receptor ($K_i \approx 1$ nM) relative to the $\beta 1$ receptor ($K_i \approx 200$ nM).

To investigate the feasibility of estimating the affinities of compounds using GPCR arrays, we studied the binding of BT-NT in the presence of unlabeled neurotensin to arrays of the neurotensin receptor. Figure 2C shows fluorescence images reflecting the concentration dependence of the inhibition. From a plot of the binding signal versus the concentration of neurotensin, we estimate IC_{50} to be ~ 2 nM, which is close to that obtained using other techniques.¹⁶ Significantly, this agreement suggests that the GPCR–G protein complex is largely preserved in the microspot,¹ which further suggests the possibility of monitoring the activation of G proteins.

The approach described here for fabricating membrane protein arrays is highly practical; binding assays on these arrays demonstrate high specificity and no apparent artifacts due to receptor immobilization. The utility of membrane microarrays goes well beyond multiplexed compound-screening—as models of the cell-surface, membrane microarrays will also enable highly parallel studies of fundamental processes such as multivalent interactions and cell–cell communication.²¹

Supporting Information Available: Details for fabrication and storage of arrays and FRAP experimental procedures (PDF). This material is available free of charge via the Internet at <http://pubs.acs.org>

References

- (1) *G Protein-Coupled Receptors*; Haga, T., Berstein, G., Eds.; CRC Press: Boca Raton, 1999.
- (2) Brown, P. O.; Botstein, D. *Nat. Genet.* **1999**, *21*, 33.
- (3) Kodadek, T. *Chem. Biol.* **2001**, *8*, 105.
- (4) (a) MacBeath, G.; Schreiber, S. L. *Science* **2000**, *289*, 1760. (b) Zhu, H. et al. *Science* **2001**, *293*, 2101.
- (5) Vogel and co-workers have described arrays of biotin-derivatized rhodopsin on patterned substrates. (*Nat. Biotechnol.* **1999**, *17*, 1105).
- (6) Drews, J. *Science* **2000**, *287*, 1960.
- (7) Unless otherwise noted, printing was carried out on ultraflat glass slides coated with GAPS.
- (8) (a) Lahiri, J.; Jonas, S. J.; Frutos, A. G.; Kalal, P.; Fang, Y. *Biomed. Microdevices* **2001**, *3*, 157. (b) Lahiri, J.; Kalal, P.; Frutos, A. G.; Jonas, S. J.; Schaeffler, R. *Langmuir* **2000**, *16*, 7805.
- (9) Arrays of GPCRs or lipids were printed using a robotic pin printer (Cartesian Technologies) with quill pins. After printing the arrays were incubated in a humid chamber at room temperature for 1 h. After ligand binding, the arrays were rinsed with water, dried, and imaged in a fluorescence scanner (GenePix 4000A or a ScanArray 5000).
- (10) Cremer, P. S.; Boxer, S. G. *J. Phys. Chem. B* **1999**, *103*, 2554.
- (11) Microspots of DPPC/DMPC, but not egg-yolk PC, are stable on Brij-derivatized self-assembled monolayers of alkanethiols on gold.⁸
- (12) Groves, J. T.; Ulman, N.; Boxer, S. G. *Science* **1997**, *275*, 651.
- (13) Shen, W. W.; Boxer, S. G.; Knoll, W.; Frank, C. W.; *Biomacromolecules* **2001**, *2*, 70.
- (14) Microspots were imaged in ambient tapping mode using a Digital Instruments NanoScope III AFM instrument.
- (15) The equivalent of ~ 5 bilayers of DLPC was printed. This calculation is based on a DLPC concentration of 1.1 mM, a printed volume of 1 nL, a microspot diameter of 200 μm , and a surface area of 45 \AA^2 per lipid molecule. AFM images of DPPC spots showed discontinuous multilayer structures (data not shown).
- (16) Barroso, S. et al. *J. Biol. Chem.* **2000**, *275*, 328.
- (17) Gold slides presenting monolayers of 11-mercaptopoundecanoic acid were derivatized with GAPS using standard carbodiimide chemistry.
- (18) Li, L.; Ruzgas, T.; Gaigalas, A. K. *Langmuir* **1999**, *15*, 6358.
- (19) Staehelin, M.; Jaeggi, K.; Wigger, N. *J. Biol. Chem.* **1983**, *258*, 3496.
- (20) Bilski, A. J.; Halliday, S. E.; Fitzgerald, J. D.; Wale, J. L. *J. Cardiovasc. Pharmacol.* **1983**, *5*, 430.
- (21) (a) Mammen, M.; Seok-Ki, C.; Whitesides, G. M. *Angew. Chem., Int. Ed.* **1998**, *37*, 2755. (b) Qi, S. Y.; Groves, J. T.; Chakraborty, A. K. *Proc. Natl. Acad. Sci. U.S.A.* **2001**, *98*, 6548.

JA017346+